A Generalized Gazi–Passino Model With Coordinate-Coupling Matrices for Swarm Formation With Rotation Behavior

Giuseppe Fedele, *Member, IEEE*, Luigi D'Alfonso, and Veysel Gazi, *Senior Member, IEEE*

***Abstract*—In this article, a kinematic continuous time swarm model is considered by extending the results in the paper "A class of attractions/repulsion functions for stable swarm aggregations" (as shown in the *International Journal of Control*, vol. 77, pages 1567–1579). The extension regards a more general class of attraction/repulsion functions that can be used to explain the formation of rotational patterns in a swarm of agents. The main characteristic of this model is the introduction of two coordinate-coupling matrices weighting both the attractive and the repulsive interactions among the agents. A stability analysis is presented to characterize the swarm in terms of size and cohesiveness. Moreover, a class of attraction/repulsion functions is presented to guarantee the cohesiveness of the swarm in a polytopic region and a steady-state motion of the agents in a rotational frame around the swarm centroid. Numerical simulations are provided to illustrate the obtained results.**

***Index Terms*—Agent-based systems, autonomous systems, cooperative control, swarms.**

I. Introduction

THE STUDY of swarm behaviors, in terms of collective dynamics of groups of autonomous mobile agents, has attracted increasing attention in recent years due to its wide use in theoretical research and engineering applications [2], [3]. These studies typically focus on analyzing how coordinated collective behavior arises as a result of local interactions among the individuals. A traditional and well-studied behavior of multiagent systems is consensus, where the goal is for the states of all agents to converge to a common desired value by implementing an appropriate protocol [4]–[6].

Manuscript received 25 May 2021; revised 1 September 2021; accepted 7 November 2021. Date of publication 6 January 2022; date of current version 19 September 2022. Recommended by Associate Editor L. Pavel. *(Corresponding author: Giuseppe Fedele.)*

Giuseppe Fedele is with the Department of Informatics, Modeling, Electronics and Systems Engineering, University of Calabria, 87036 Rende, Italy (e-mail: giuseppe.fedele@unical.it).

Luigi D'Alfonso is with the GiPStech s.r.l., 87036 Rende, Italy (e-mail: l.dalfonso@gipstech.com).

Veysel Gazi was with the Department of Electrical and Electronics Engineering, Faculty of Engineering, Marmara University, 34722 Istanbul, Turkey. He is now with the Faculty of Electrical and Electronics Engineering, Department of Control and Automation Engineering, Davutpasa, Esenler, 34220 Istanbul, Turkey (e-mail: vgazi@yildiz.edu.tr).

Digital Object Identifier 10.1109/TCNS.2022.3141012

This problem arises in a number of applications, such as swarming, schooling, flocking, or rendezvous, and for this reason, it can be regarded as fundamental for other forms of swarm system control. The consensus can be regarded as the fundamental step for solving other control problems for swarm systems: the formation problem where the aim is to control agents to form and maintain some relative positions or a prescribed shape [7]; flocking where agents reach a cohesiveness from their initial positions and move in the same direction at the same speed [8], [9]; and consensus/cohesion tracking where a group of agents self-organizes to track a reference trajectory [10], [11].

Far from being exhaustive due to the vast amount of literature on formation control, only some of the most commonly used methodologies to achieve the formation of a cohesive or aggregated swarm are briefly described here. Generally speaking, control strategies for multiagent systems may be divided into two categories: 1) the centralized scheme and 2) the distributed one. In the centralized scheme, a central processing unit is in charge to monitor the coordination of the team in order to accomplish the formation task based on the information gathered from all agents. Conversely, in a distributed control architecture, the agents can communicate and share information with neighboring members without the aid of a central unit. While the centralized scheme lacks robustness in the case of failure of the central unit, the distributed systems are more robust and scalable [12]. In formation control for a group of coordinated agents, different control topologies can be adopted depending on the specific scenarios: Artificial potential field, behavior-based formation control, leader–follower, and virtual structure methods, just to name a few.

The most widely used approach in the formation control is the *artificial potential field method*, which generates repulsive/attractive forces for mobile agents to avoid collisions and maintain distances among them. The idea of using potential functions for the specification of robot tasks was pioneered by Khatib [13] and used in a plethora of papers in order to specify interagent interactions and interactions of the agents with their environment.

Another common method is the *leader–follower approach*, where a physical or virtual leader is considered to define actions for the other agents [14], [15]. These actions are obtained through interaction among neighbors [16] or interaction with the leader [17]. Two basic types of feedback controller for

maintaining the formation are usually exploited [18]: 1) the $l-\psi$ controller, whose aim is to maintain a desired length and a desired relative angle between the leader and the follower and 2) the $l-l$ controller that considers the relative position of three agents and maintain the desired lengths between them. The *behavior-based control* for swarm formation, first introduced in [19], considers a set of predefined basic behaviors, such as obstacle avoidance, formation keeping, and goal seeking. The final control command is then determined as the sum of such basic behaviors weighted by distinct gains, which represent the desired behavior response to sensory input [20].

In [21], the *virtual structure approach* is proposed to address the problem of the maintenance of a geometric configuration during movement. The swarm is then considered as a collection of elements, which maintain a rigid relationship to each other and to a reference frame. The shape of the formation is then organized as a rigid body and obtained, at the first stage, by matching the physical position of the formation to the position of the virtual body [22].

There are also many other methods in the application of formation control. For example, in [23] and [24], a method relying on concepts from differential geometry is proposed to face the problem of controlling a large number of robots. Such a method permits to derive controls for the single agents by first defining the macroscopic behavior or characteristics of the swarm. More recently, a novel distributed model-predictive control architecture is proposed in [25], where a model for swarm formation is jointly exploited within a model-predictive control framework to reduce as much as possible the use of on-board sensors in long-range missions of autonomous vehicles.

A very recent survey and application-focused atlas of collective behavior coordination algorithms for the multiagent system can be found in [26].

Recently, the problem of investigating swarm models for a rotating formation in multiagent systems has received considerable attention [27]. Many circular motion phenomena occur in nature, such as celestial motion and Earth orbiting satellites. The circular group movement is a typical example of collective behavior also observed in a wide range of biological systems. Some Paenibacillus species, for example, can exhibit complex pattern forming behavior. A kind of Paenibacillus, *P. vortex*, is so named because of the vigorous rotation of entire colonies and of areas within colonies [28].

Other microorganism colonies, such as *Escherichia coli* bands, exhibit a nontrivial macroscopic behavior. In particular, when the cells are close to a solid surface, they trace out circular trajectories [29]. Moreover the bacteria within the colonies growing on wet agar surfaces produce turbulent as well as rotating motions [30]. In [31], based on simple assumptions directly related to the experimental observations on colony formation under various conditions, a one-dimensional model is developed to characterize the self-organized collective behavior of a large number of bacteria *Proteus mirabilis* that develop a series of concentric rings, when inoculated on the surface of a suitable hard agar medium.

A circular behavior is also known in animal aggregations. In [32], the swirling motion in groups of *Daphnia Magna* is studied showing that vortex formation is induced by sending a light beam vertically into the water. To this aim, a model is designed that contains an active motion, a weak attractive force toward the light beam, and mutual repulsion between the Daphnia. Another example can be found in [33], where collective vortex formation by congeneric spadefoot toad tadpoles, *Spea bombifrons* and *Spea multiplicata*, is observed in laboratory experiments. The transitions in the social behavior and collective motion of the marine flat worm *Symsagittifera roscoffensis* renowned as the plant-animal are studied in [34], where a model is proposed to show how individual worms move, how small groups of worms interact with one another, and how circular mills form. These circular mills eventually lead to such high densities that the worms can form continuous biofilms and, thus, act as if they are a superorganismic seaweed. In many cases, the function of these aggregations remains unknown as in the schools of up to 50 basking sharks *Cetorhinus maximus* observed in the southern Gulf of Maine from early September through mid-October 2002 [35], which exhibit a variety of schooling patterns, including echelon, cartwheel, and milling formations. Indeed, the absence of potential predators in the area suggests that it is not an antipredation response but maybe a group courtship behavior.

Among the models proposed in the relevant literature, one of the earliest contributions can be found in [36], where a virtual leader is used to manipulate group geometry and direct the motion of the group. In the particular case of a stationary virtual leader, a rotating swarm behavior can be obtained. Using the same arguments, applied to a model of all-to-all coupled identical particles moving in the plane at unit speed, in [37], a design methodology to stabilize isolated relative equilibria corresponding to circular motion of all particles with fixed relative phases is proposed. In [38], it is shown that collective motions, including rendezvous, circular patterns, and logarithmic spiral patterns, can be achieved by introducing Cartesian coordinate coupling to the existing consensus algorithms. As a drawback, this model requires very strict conditions on the control parameters and the graph topology to ensure that agents move on circular orbits. Other works consider the motion on spherical orbits or spherical formation tracking [39], [40], where specific agent dynamics are considered for tracking given orbits on a sphere [39] or combination of pitch and yaw velocities together with surge acceleration is used for formation tracking on a sphere [40].

It is worth to underline that there is no definitive and generally applicable definition of rotational movements. On the other hand, there is a lot of interest in identifying the common causes or fundamental principles underlying this behavioral phenomenon [41]. For these reasons, based on the results presented in [1], in this article, a generalized model is proposed to explain the collective rotation of the individuals in one direction. The choice to refer to the results in [1] is not accidental. In fact, Gazi and Passino [1] investigate the properties of a simple model describing swarm aggregation on the basis of the general understanding in biology, where swarming behavior can be analyzed in terms of an interplay between a long-range attraction and a short-range repulsion among the individuals. However, the model is not able to explain the mechanisms of rotational behavior [3].

The idea exploited in this article consists of weighting these two terms (attraction–repulsion) by two matrices that couple the coordinate components of each agent. The approach has been already used in [27], where a model for vortex formation is proposed. However, the model in [27] is not so general: it requires an external reference trajectory (virtual leader) known to all the agents and a specific interaction term. The presence of the virtual leader makes emerging swarm behavior unnatural although it permits to synthesize scalable control laws that are simple at the individual level [36].

In contrast, in this article, the interaction is through a general class of attraction–repulsion functions that capture most of the attraction and repulsion forces between individuals in nature, biology, etc. In fact, many different functions satisfy the conditions of the considered class [1], [3] and are in line with the actual understanding of collective behavior mechanisms, according to which the interactions between the units can be simple (attraction/repulsion) or more complex (combinations of simple interactions) and can occur between neighbors in space or in an underlying network [42].

In this sense, the model here presented is general; it holds for any finite-dimensional space and guarantees that the centroid of the swarm members is stationary and imposes slight restrictions on the choice of the coupling matrices in the interaction terms. Such coupling matrices provide degrees of freedom to the swarm and allow us to model the overall emergent rotational behavior in engineering and natural swarms, also giving the flexibility, with an appropriate choice of the potential function parameters, to prespecify the axis and speed of rotation. Furthermore, by particular choice of these interaction matrices, the swarm can exhibit static configuration at the steady state in terms of cohesiveness: ball, polytopes, hyperplanes.

Finally, unlike the above cited papers implementing ad-hoc models to obtain only collective rotational behaviors or capable of interpreting experimental data, the method here proposed is general, since it is based on a very general class of attraction/repulsion functions, and it is more flexible since it permits to modify the swarm behavior by changing *on the fly* the coordinate-coupling matrices of the model. Indeed, such matrices represent free parameters of the swarm model, and their tuning gives a simple way to readjust and reorganize the formation based on the task under consideration.

This work constitutes the first study for the given model with that respect.

The remainder of this article is organized as follows. Section II presents the problem formulation together with a brief glimpse to graph theory. The new model and its main properties are analyzed in Section III. The rotational behavior of the swarm is proven in Section IV. Section V contains some numerical results. Finally, Section VI concludes this article.

Notations

Define with $\mathcal{M}$ the set of $d \times d$ matrices with real elements. Consider $P \in \mathcal{M}$ and denote as $P^s = 1/2(P + P^T)$ the symmetric part of P. Let $S \in \mathcal{M}$ with $S = S^T$ and denote with $\lambda_i(S)$ the ith eigenvalue of S. In addition, denote as $\lambda_{\max}(S) = \max_{i=1,\ldots,d} \lambda_i(S)$ and $\lambda_{\min}(S) = \min_{i=1,\ldots,d} \lambda_i(S)$ the maximum and minimum eigenvalue of S, respectively. The identity matrix in $\mathcal{M}$ is indicated as $\mathbb{I}_d$. A column vector of dimension n with all entries equal to 1 is indicated with $\mathbb{1}_n$, while a column vector with all the elements equal to zero with $\mathbb{0}_n$. $\mathbb{R}^+$ denotes the set of positive real numbers. $\mathcal{B}(c, r)$ with $c \in \mathbb{R}^n$ is the ball of center c and radius $r \in \mathbb{R}^+$, i.e., $\mathcal{B}(c, r) = \{z \in \mathbb{R}^n : ||z - c|| \leq r, \}$. Given a finite set $F \subset \mathbb{R}^q$, $|F|$ is its cardinality. $||\cdot||$ denotes the 2-norm operator.

II. Problem Formulation

Consider a group of n agents whose positions at time $t \geq 0$ are denoted by $z_i(t) \in \mathbb{R}^d,\ i = 1, 2, \ldots, n$. The dynamic model of each agent is described by the single integrator

$$\dot{z}_i(t) = u_i(t), \quad i = 1, 2, \ldots, n \tag{1}$$

where $u_i(t) \in \mathbb{R}^d$ is the control protocol to be designed so that the agents aggregate in a hyperball $\mathcal{B}(\bar{z}, \rho)$, where

$$\bar{z} = \frac{1}{n} \sum_{i=1}^{n} z_i(t)$$

is the centroid of the swarm members, aggregate in an imposed polytopic region, or start a rotating behavior around $\bar{z}$ by choosing a fixed axis of rotation and speed.

Note that although the single-integrator model in (1) is simple, it is very relevant since the results obtained for that model can be easily applied and recovered for swarms composed of agents with specific dynamics such as fully actuated agents with model uncertainties and nonholonomic agents with model uncertainties [3]. In fact, the advantage of the single-integrator model is to be general and independent from the specific agent dynamics. With this respect, it can serve as a reference trajectory generator for systems composed of specific agent dynamics.

A. Preliminaries

Throughout this article, a swarm of n agents is modeled as a graph. Specifically, agents are represented as nodes of the graph, and interactions due to sensing and communication are represented as edges of the graph. An undirected graph is a set $\mathcal{G} = \{V, E\}$, where $V = \{1, \ldots, n\}$ is a nonempty finite set of nodes, one for each agent of the swarm, and $E \subseteq \{(i, j) : i, j \in V,\ i \neq j\}$ is a set of unordered pairs of vertices. The set of neighbors of the ith agent is denoted by $\mathcal{N}_i = \{j \in V \backslash \{i\} : (i, j) \in E\}$. The graph $\mathcal{G}$ is complete if there is an edge for each pair of nodes. $\mathcal{G}$ is encoded by the Laplacian matrix $\mathcal{L}_\mathcal{G} = \Delta_\mathcal{G} - A_\mathcal{G}$. The matrix $A_\mathcal{G}$ is the adjacency matrix defined as

$$A_\mathcal{G}(i, j) = \begin{cases} 1, & \text{if } (i, j) \in E \\ 0, & \text{otherwise} \end{cases}$$

$i, j = 1, 2, \ldots, n$. $\Delta_\mathcal{G} = \text{diag}(\Delta_1, \Delta_2, \ldots, \Delta_n)$ is the diagonal degree matrix, where $\Delta_i = |\mathcal{N}_i|$ is the degree of the ith agent. Let $\Delta_{\mathcal{G},\max} = \max_{i=1,2,\ldots,n} \Delta_i$ be the maximum degree among all agents. Some properties of $\mathcal{L}_\mathcal{G}$ are important for the analysis of aggregation characteristics of the swarm [43].

1) $\mathcal{L}_\mathcal{G}$ has at least one zero eigenvalue with the associated eigenvector $\mathbb{1}_n$.
2) $\mathcal{L}_\mathcal{G}$ has a simple zero eigenvalue if and only if the corresponding graph is connected.
3) The quadratic form
$$z^T\left(\mathcal{L}_\mathcal{G}\otimes\mathbb{I}_d\right)z=\sum_{(i,j)\in E}||z_i-z_j||^2$$
where $z=[z_1^T,\ldots,z_n^T]^T$ and $\otimes$ denotes the Kronecker product, is positive semidefinite.
4) For a connected graph, the second smallest eigenvalue $\lambda_2(\mathcal{L}_\mathcal{G})>0$; moreover, one has that
$$\min_{||x||\neq 0,\ \mathbb{1}_n{}^T x=0}\frac{x^T\mathcal{L}_\mathcal{G}x}{x^Tx}=\lambda_2(\mathcal{L}_\mathcal{G})>0.$$
Therefore, $x^T\mathcal{L}_\mathcal{G}x\geq\lambda_2(\mathcal{L}_\mathcal{G})||x||^2\ \forall x\in\mathbb{R}^n$, such that $||x||\neq 0$ and $\mathbb{1}_n{}^T x=0$; note that these are the nonzero vectors, which are orthogonal to $\mathbb{1}_n$.
5) If the graph is complete, i.e. $\mathcal{N}_i=\{V\backslash\{i\}\}, i=1,\ldots,n$ then $\lambda_1(\mathcal{L}_\mathcal{G})=0,\ \ \lambda_2(\mathcal{L}_\mathcal{G})=\cdots=\lambda_n(\mathcal{L}_\mathcal{G})=n,$ and $\Delta_{\mathcal{G},\max}=n-1$.

These properties will be used throughout the following sections.

III. Swarm Model and Properties

Gazi and Passino [1] proposed a simple swarm model that consists of a number of individuals (or members) with the same attraction–repulsion role and with identical interaction strength among the individuals. They have shown that the model, based on artificial potential field methods, can capture the basic features of aggregation, cohesion, and stability of a swarm. Such properties are of interest in formation control and distributed optimization problems. The control protocol of an individual agent is chosen as
$$u_i(t)=\sum_{j\in\mathcal{N}_i}g(z_i(t)-z_j(t)) \tag{2}$$
where $g(\cdot):\mathbb{R}^d\to\mathbb{R}^d$ represents the interaction force between the corresponding agents, and it is assumed to have a long-range attraction and short-range repulsion nature. According to [1], some properties were proven [3] in the case of complete graph.

1) the centroid $\bar{z}$ of the swarm is stationary over time.
2) the swarm moves toward and remains within a bounded region.
3) the swarm reaches the bounded region in finite time.
4) the swarm converges to a steady-state configuration.

These properties are satisfied if the following assumptions holds.

Assumption 1: The attraction–repulsion function $g(\cdot)$ is of the form
$$g(y)=-y\left(g_a(||y||)-g_r(||y||)\right) \tag{3}$$
where $g_a:\mathbb{R}^+\to\mathbb{R}^+$ represents the magnitude of the attraction term and has a long range, whereas $g_r:\mathbb{R}^+\to\mathbb{R}^+$ represents the magnitude of the repulsion term and has a short range.

Assumption 2: There exists a unique distance δ at which $g_a(\delta)=g_r(\delta)$. Moreover, $g_a(||y||)>g_r(||y||)$ for $||y||>\delta$ and $g_r(||y||)>g_a(||y||)$ for $||y||<\delta$;

Assumption 3: The attraction and the repulsion terms $g_a(||y||)$ and $g_r(||y||)$ are chosen such that there exist corresponding functions $J_a, J_r:\mathbb{R}^+\to\mathbb{R}$, for which one has
$$\bigtriangledown_y J_a(||y||)=yg_a(||y||),\quad \bigtriangledown_y J_r(||y||)=yg_r(||y||).$$

The kinematic model (3), however, is not able to describe the swarm behavior in some engineering applications, where individuals never stop, like the more complicated movement where agents self-organize starting a rotating motion in a single direction, neither to describe some pattern formation in swarms of biological entities.

In order to overcome this drawback, in this article, the attraction–repulsion function is modified as
$$g(y)=-g_a(||y||)Hy+g_r(||y||)My \tag{4}$$
where $H, M\in\mathcal{M}$ denote Cartesian-coordinate-coupling matrices.

Unlike the model in [1], the presence of the two matrices H and M introduces some degrees of freedom in the swarm dynamics, as exploited in the remainder of this article. If the matrices H and M are chosen as $\mathbb{I}_d$, then the model (1) with (2) and (4) becomes the proposed one in [1].

The idea of using matrices to couple agents' coordinates is not new. In [38], for example, the collective motions of a team of vehicles with double-integrator dynamics are investigated by considering the introduction of a rotation matrix to an existing consensus algorithm. Moreover, in [10], some properties of these matrices are exploited in order to obtain several static configurations or rotating behaviors in the steady state for a restricted class of swarm models without general attraction–repulsion functions. The results in this article are more general and applicable to a larger class of systems. The main characteristics of the new model are shown below. In particular, the same results derived in [1] are extended taking into account the presence of the two weight matrices and the assumption of connected, but not necessarily complete, graph.

Lemma 1: The centroid $\bar{z}$ of the swarm described by the model (1), (2), (4) is stationary for all t.

Proof: The reciprocity of interactions in (2) guarantees that $\sum_{i=1}^n u_i(t)=\mathbb{0}_d\,\forall t$. Therefore, the quantity $\sum_{i=1}^n \dot{z}_i(t)$ is equal to $\mathbb{0}_d$ for all time instants, and the proof follows. ■

As the first step, the stability analysis of swarm cohesion is investigated exploiting the tendency of each member to move toward the centroid of the swarm. The aggregating behavior of the swarm is considered in the two scenarios of bounded and unbounded repulsion. To this aim, the Lyapunov function
$$V=\frac{1}{2}\sum_{i=1}^N e_i^Te_i$$
is chosen as the candidate to specify the ultimate bound of the swarm, where $e_i:=z_i-\bar{z}$. Since from Lemma 1, we have $\dot{\bar{z}}=\mathbb{0}_d$, for each individual i, the time derivative of the distance from

the centroid can be written as follows:

$$\dot{e}_i = -\sum_{j\in\mathcal{N}_i} \left[g_a(||e_i - e_j||)H - g_r(||e_i - e_j||)M\right](e_i - e_j).$$

Taking the time derivative of V, we obtain $\dot{V} = \dot{V}_1 + \dot{V}_2$ with

$$\dot{V}_1 = -\sum_{i=1}^{n}\sum_{j\in\mathcal{N}_i} g_a(||e_i - e_j||)e_i^T H(e_i - e_j)$$

$$\dot{V}_2 = \sum_{i=1}^{n}\sum_{j\in\mathcal{N}_i} g_r(||e_i - e_j||)e_i^T M(e_i - e_j).$$

A. Bounded Repulsion

In this section, we consider the case in which the repulsive term is constant or bounded and the attraction is bounded from below.

Theorem 1: Consider the swarm described by the model (1), (2), (4) with constant or bounded repulsion $g_r(||y||)||y|| \leq \beta$ and linearly bounded from below attraction $g_a(||y||) \geq \alpha$ for some $\alpha, \beta \in \mathbb{R}^+$. Let $H^s > 0$ and assume that the graph $\mathcal{G}$ is connected; then, the swarm moves toward and remains within a bounded region $\mathcal{B}(\bar{z}, r)$ with

$$r = \frac{\beta\Delta_{\mathcal{G},\max}||M||\sqrt{n}}{\alpha\lambda_{\min}(H^s)\lambda_2(\mathcal{L}_\mathcal{G})}. \tag{5}$$

Proof: The term $\dot{V}_1$ can be restated with respect to (w.r.t.) the set of the edges E and bounded as

$$\dot{V}_1 = -\sum_{(i,j)\in E} g_a(||e_i - e_j||)(e_i - e_j)^T H(e_i - e_j)$$
$$\leq -\alpha\lambda_{\min}(H^s)\sum_{(i,j)\in E}||e_i - e_j||^2.$$

By using the properties of the Laplacian matrix recalled in Section II, it follows that

$$\dot{V}_1 \leq -\alpha\lambda_{\min}(H^s)e^T(\mathcal{L}_\mathcal{G}\otimes\mathbb{I}_d)\,e \leq -\alpha\lambda_{\min}(H^s)\lambda_2(\mathcal{L}_\mathcal{G})||e||^2 \tag{6}$$

where $e = [e_1^T, \ldots, e_n^T]^T$. Here, the second inequality follows from the fact that the vector $v_j \triangleq [e_1(j), \ldots, e_n(j)]^T \in \mathbb{R}^n$ containing the jth component of each vector e_i, $i = 1, \ldots, n$, is such that $v_j^T\mathbb{1}_n = 0\ \forall\ j = 1, \ldots, d$. This, on the other hand, stems from the fact that agents are not at consensus and that interactions are reciprocal. Due to the repulsive component of the interaction function, the consensus steady state could be achieved only if all the agents were originally located at the same point. Similarly, the second term $\dot{V}_2$ can be bounded as

$$\dot{V}_2 \leq \sum_{i=1}^{n}||e_i||\,||M||\sum_{j\in\mathcal{N}_i} g_r(||e_i - e_j||)||e_i - e_j||.$$

Note that from the hypothesis of bounded repulsion, it follows that

$$\sum_{j\in\mathcal{N}_i} g_r(||e_i - e_j||)||e_i - e_j|| \leq \beta\Delta_{\mathcal{G},\max}.$$

Therefore, we have

$$\dot{V}_2 \leq \beta\Delta_{\mathcal{G},\max}||M||\sqrt{n}||e|| \tag{7}$$

where the inequality $\sum_{i=1}^{n}||e_i|| \leq \sqrt{n}||e||$ has been used. Substituting (6) and (7) into $\dot{V}$, we obtain

$$\dot{V} \leq -\alpha\lambda_{\min}(H^s)\lambda_2(\mathcal{L}_\mathcal{G})||e||^2 + \beta\Delta_{\mathcal{G},\max}||M||\sqrt{n}||e||$$

which implies that $\dot{V}$ is negative definite if the following holds:

$$||e|| \geq \frac{\beta\Delta_{\mathcal{G},\max}||M||\sqrt{n}}{\alpha\lambda_{\min}(H^s)\lambda_2(\mathcal{L}_\mathcal{G})}$$

and the motion of the swarm is uniformly bounded within the region $\mathcal{B}(\bar{z}, r)$. ■

Remark 1: If the graph is complete, i.e., $\Delta_{\mathcal{G},\max} = n - 1$, $\lambda_2(\mathcal{L}_\mathcal{G}) = n$, then the bound given by (5) becomes

$$||z_i - \bar{z}|| \leq \frac{\beta||M||(n-1)\sqrt{n}}{\alpha\lambda_{\min}(H^s)n}. \tag{8}$$

B. Unbounded Repulsion

Here, we consider the case of unbounded repulsion for infinitesimally small arguments. As in the previous scenario, the attraction is assumed to be linearly bounded from below. We assume that the norm of the repulsive term is unbounded and satisfies the inequality $g_r(||y||)||y|| \leq \beta/||y||$, which means that as $||y|| \to 0$, $g_r(||y||)||y|| \to \infty$, but grows slower than the term $\beta/||y||$.

Theorem 2: Consider the swarm described by the model (1), (2), (4) with unbounded repulsion $g_r(||y||)||y|| \leq \beta/||y||$ and linearly bounded from below attraction $g_a(||y||) \geq \alpha$ for some $\alpha, \beta \in \mathbb{R}^+$. If $H^s > 0$, $M^s \geq 0$ and the graph $\mathcal{G}$ is connected, then the swarm moves toward and remains within a bounded region $\mathcal{B}(\bar{z}, r)$ with

$$r = \sqrt{\frac{\beta\lambda_{\max}(M^s)|E|}{\alpha\lambda_{\min}(H^s)\lambda_2(\mathcal{L}_\mathcal{G})}}. \tag{9}$$

Proof: Following the same lines of Theorem 1, the term $\dot{V}_1$ is bounded as in (6), while $\dot{V}_2$ can be bounded as follows:

$$\dot{V}_2 \leq \beta\lambda_{\max}(M^s)|E|.$$

Finally, $\dot{V}$ is negative definite if

$$||e||^2 > \frac{\beta\lambda_{\max}(M^s)|E|}{\alpha\lambda_{\min}(H^s)\lambda_2(\mathcal{L}_\mathcal{G})}$$

and then each individual moves toward the region

$$||z_i - \bar{z}|| \leq \sqrt{\frac{\beta\lambda_{\max}(M^s)|E|}{\alpha\lambda_{\min}(H^s)\lambda_2(\mathcal{L}_\mathcal{G})}}.$$

■

Remark 2: In the case of a complete graph, the number of edges is $|E| = n(n-1)/2$, $\lambda_2(\mathcal{L}_\mathcal{G}) = n$; then, the bound (9) becomes

$$||z_i - \bar{z}|| \leq \sqrt{\frac{\beta\lambda_{\max}(M^s)(n-1)}{2\alpha\lambda_{\min}(H^s)}}. \tag{10}$$

Note that these bounds are conservative and the actual swarm size is smaller than the obtained bounds. Moreover, if $M^s > 0$, then the collision avoidance among agents is ensured.

C. Cohesion in a Polytopic Region

Previous results can be specialized in order to guarantee the cohesion of the agents in a polytopic region centered at the swarm centroid.

Corollary 1: Let $z_{i,k}$ and $\bar{z}_k$ be the kth coordinate, with $k = 1, \ldots, d$, of the ith agent and of the swarm centroid, respectively. If the matrices H and M are chosen as $H = \mathbb{I}_d$ and $M = Q^T \Lambda Q$ with $Q^T Q = Q Q^T = \mathbb{I}_d$ and $\Lambda = \text{diag}(\lambda_1, \ldots, \lambda_d)$, $\lambda_i \geq 0, i = 1, \ldots, d$, then the agents enter the polytopic region:

1) in the bounded repulsion case:

$$|z_{i,k} - \bar{z}_k| \leq \frac{\lambda_k \beta \Delta_{\mathcal{G},\max} \sqrt{n}}{\alpha \lambda_2 (\mathcal{L}_\mathcal{G})} \tag{11}$$

2) in the unbounded repulsion case:

$$|z_{i,k} - \bar{z}_k| \leq \sqrt{\frac{\lambda_k \beta |E|}{\alpha \lambda_2 (\mathcal{L}_\mathcal{G})}}. \tag{12}$$

Proof: Since the matrix Q is unitary, then by making the change of variable $z_i = Q^T y_i$, the swarm model can be rewritten as

$$\dot{y}_i = -\sum_{j \in \mathcal{N}_i} \left[g_a(||y_i - y_j||) - g_r(||y_i - y_j||) \Lambda \right] (y_i - y_j).$$

The proof follows by using the same arguments of Theorems 1 and 2 for the Lyapunov function $V = \frac{1}{2} \sum_{i=1}^n (y_{i,k} - \bar{y}_k)^2$, where $\bar{y} = Q\bar{z}$. ■

Remark 3: The results in Corollary 1 can be extended to similar matrices obtained by M through a rotation matrix R. In this case, the steady-state configuration will be rotated too w.r.t. the original one without modification of the mutual distances between agents. In particular, if the swarm is ensured to be driven into a given bounded region using M, then it will go into the same region but rotated by R, if the M is changed in RMR^T.

Remark 4: The interaction imposed by the matrix M can be easily tuned to modulate the repulsion among agents on the d-axis. In particular, if $M = \mu \mathbb{I}_d, \mu \geq 0$, the interaction is uniformly distributed on the d dimensions. From a general point of view, the repulsion modulated by M is related to its eigenvalues, and the greater the module of an eigenvalue, the stronger the interaction imposed on the related eigenspace.

IV. Rotating Behavior

When agents are inside the bounded region $\mathcal{B}(\bar{z}, r)$, it is possible to obtain a rotational behavior around the swarm centroid by appropriately choosing the parameters of the model (1), (2), (4), i.e., the attraction/repulsion functions and the matrices H and M in (4). In order to investigate the capabilities of the proposed swarm model to obtain a rotating behavior, for the sake of the reader, the following arguments are exploited [44].

Special Orthogonal group $SO(d)$:

$$SO(d) = \left\{ Q \in \mathcal{M} : \ det(Q) = 1, \ QQ^T = Q^T Q = \mathbb{I}_d \right\}.$$

$SO(d)$ is a group, where $\mathbb{I}_d$ is the neutral element. Moreover, the multiplication and the inversion are both smooth. This makes $SO(d)$ a manifold of the set of matrices $\mathbb{R}^{d \times d}$ (Lie group). The dimension of $SO(d)$ is $d(d-1)/2$, and it leaves a d-dimensional sphere invariant. Therefore, the matrices in $SO(d)$ are rotation matrices. Let us consider a rotation matrix $R \in SO(d)$ representing the relative orientation of an object w.r.t. an inertial frame. If R is a time-varying matrix, meaning that the relative orientation of the object is changing with time, its time derivative can be expressed as $\dot{R} = RA$, where the matrix A represents the so-called *angular velocity matrix*. It is a skew-symmetric matrix, whose elements are composed of the elements of the angular velocity vector leading to the time change in R. From the above equality, the matrix A can be written as $A = R^T \dot{R}$. For example, consider the case of $SO(3)$. If an object rotates with angular velocity vector $\omega_A = (\omega_x, \omega_y, \omega_z)^T$ about an inertial frame, the corresponding angular velocity matrix is given by

$$A = \begin{pmatrix} 0 & -\omega_z & \omega_y \\ \omega_z & 0 & -\omega_x \\ -\omega_y & \omega_x & 0 \end{pmatrix}.$$

Note that both A and ω_A define the axis of rotation, the direction of rotation (based on the right-hand rule), and the speed of rotation (the magnitude of the vector) for $d \geq 3$ (the case $d = 2$ corresponds to a rotation around an axis orthogonal to the 2-D plane). In fact, if $u \in \mathbb{R}^d$ is the rotation axis, it must satisfy $Ru = u \ \forall t$, from which $RAu = \mathbb{0}_d$ Therefore, the product Au is equal to $\mathbb{0}_d$ and u is parallel to the vector defining A.

A. Case of the Attraction Only With the Skew-Symmetric Coordinate-Coupling Matrix A

Let us consider the particular case with

$$g_a(||y||) = \rho = \text{const.}, \ g_r(||y||) = 0, \ H = A$$

and then the model

$$\dot{z}_i(t) = -\rho \sum_{j \in \mathcal{N}_i} A(z_i(t) - z_j(t)), \ z_i(t) \in \mathbb{R}^3. \tag{13}$$

The model (13) has interesting properties. First, it is easy to note that the swarm evolution occurs on planes perpendicular to the axis of rotation ω_A. In fact, by considering the function $f_i = \frac{1}{2}(\omega_A^T z_i)^2$, it follows that

$$\dot{f}_i = -\rho(\omega_A^T z_i) \sum_{j \in \mathcal{N}_i} \omega_A^T A(z_i - z_j) = 0.$$

Moreover, the swarm dynamics is cohesive; this follows by considering the Lyapunov function

$$V = \frac{1}{2} \sum_{i=1}^n z_i^T z_i$$

whose derivative

$$\dot{V} = -\rho \sum_{(i,j) \in E} (z_i - z_j)^T A (z_i - z_j) = 0$$

reveals that $V =$ constant and then $||z_i|| \leq \sqrt{2\,V}\ \forall i$.

The overall system can be represented in matrix form by

$$\dot{z}(t) = -\rho Q z(t) \tag{14}$$

where $Q = \mathcal{L}_\mathcal{G} \otimes A$ and $z(t) = (z_1^T(t), ..., z_n^T(t))^T$. Assuming that the graph is connected, then the spectrum of the Laplacian assumes the form

$$0 = \lambda_1(\mathcal{L}_\mathcal{G}) < \lambda_2(\mathcal{L}_\mathcal{G}) \leq \cdots \leq \lambda_n(\mathcal{L}_\mathcal{G}).$$

The skew-symmetric matrix A has a null eigenvalue and a pair of conjugated complex eigenvalues $\pm\jmath||\omega_A||$. Then, the spectrum of the matrix Q is

$$\left\{ \underbrace{0}_{n+2}, \underbrace{\pm\jmath\lambda_2(\mathcal{L}_\mathcal{G})||\omega_A||, \ldots, \pm\jmath\lambda_n(\mathcal{L}_\mathcal{G})||\omega_A||}_{2(n-1)} \right\}.$$

Moreover, the matrix Q is skew symmetric since

$$\mathcal{L}_\mathcal{G} \otimes A + (\mathcal{L}_\mathcal{G} \otimes A)^T = \mathcal{L}_\mathcal{G} \otimes A + \mathcal{L}_\mathcal{G}^T \otimes A^T = 0_{3n}$$

from which it follows that the exponential matrix e^Q is orthogonal. Additionally, $det(e^Q) = 1$, so e^{Qt} is a rotation matrix for each $t \in \mathbb{R}$. Consider the singular value decomposition of Q, i.e., $Q = USV^T$ with $U, V \in \mathbb{R}^{3n\times 3n}$ orthogonal matrices; then, we have

$$\Sigma = U^T Q U = \begin{pmatrix} E_1 & \cdots & & \\ \vdots & \ddots & \vdots & \\ & \cdots & E_{n-1} & \\ \cdots & & & 0_{n+2} \end{pmatrix}$$

where each block E_i is a real 2-D matrix of the form

$$E_i = \theta_i \begin{pmatrix} 0 & -1 \\ 1 & 0 \end{pmatrix}$$

with $\theta_i = \lambda_{i+1}(\mathcal{L}_\mathcal{G})||\omega_A||$, $i = 1, \ldots, n-1$ [45]. By the change of coordinates $y(t) = U^T z(t)$, (14) becomes

$$\dot{y}(t) = -\rho\Sigma y(t).$$

Therefore

$$y(t) = e^{-\rho\Sigma t} y(0)$$

where $e^{-\rho\Sigma t}$ has a block structure

$$\begin{pmatrix} e^{-\rho E_1 t} & \cdots & & \\ \vdots & \ddots & \vdots & \\ & \cdots & e^{-\rho E_{n-1} t} & \\ \cdots & & & 1_{n+2} \end{pmatrix}$$

and the generic block is

$$e^{-\rho E_i t} = \begin{pmatrix} \cos(\rho\theta_i t) & \sin(\rho\theta_i t) \\ -\sin(\rho\theta_i t) & \cos(\rho\theta_i t) \end{pmatrix}.$$

The above derivations can be summarized in the following result.

Theorem 3: Consider the swarm model (1), (2), (4) with

$$g_a(||y||) = \rho = \text{constant},\ g_r(||y||) = 0, \omega_A = (\omega_x, \omega_y, \omega_z)^T,$$

$$H = A = \begin{pmatrix} 0 & -\omega_z & \omega_y \\ \omega_z & 0 & -\omega_x \\ -\omega_y & \omega_x & 0 \end{pmatrix}$$

and $d = 3$. Then, the swarm will be bounded and reach a dynamic configuration, where agents rotate around the axis rotation defined by ω_A (viz. the matrix A) passing through the swarm centroid. Moreover, the motion will occur on planes perpendicular to the axis of rotation, and the movement of each agents results in a sum of sin/cos signals at frequencies $\rho\lambda_k(\mathcal{L}_\mathcal{G})||\omega_A||,\ k = 2, \ldots, n$.

Remark 5: Note that, given desired axis and direction of rotation, one can easily determine the vector ω_A and construct the corresponding skew-symmetric matrix A. Moreover, the speed of rotation depends both on the magnitude of ω_A and the connectivity of the interaction graph $\mathcal{G}$ through the eigenvalues of the graph Laplacian. Therefore, with different graph topologies, different speeds can be achieved for the individual agents. Moreover, the rotation speeds can be scaled by scaling the angular velocity vector ω_A.

B. Case of Complete Graph

In this section, we investigate sufficient conditions to guarantee common rotational behavior of the swarm, i.e., conditions under which each individual rotates, with the same angular velocity, around a common axis of rotation passing through the swarm centroid. This means that it is possible to make a time-varying change of variable by using a rotation matrix R related to the skew-symmetric matrix A, i.e., $R = e^{At}$. The swarm achieves a rotational movement if the agents reach fixed steady-state positions in the rotating reference frame. This idea is exploited in the following theorem, where conditions on the coupling matrices H and M and on the interaction functions $g_a(||\cdot||)$ and $g_r(||\cdot||)$ are given.

Theorem 4: Consider the swarm model (1), (2), (4) with Assumptions 1–3 satisfied. If the graph $\mathcal{G}$ is complete, the attractive term is chosen as $g_a(||y||) = 1/n$ and the matrices $M = S - A$ and $H = S$ with $S = S^T > 0$ and $A = -A^T$, then the swarm will reach a dynamic configuration, where agents rotate around the swarm centroid with rotation axis and angular velocity defined by the matrix A.

Proof: Consider a reference frame rotating around the swarm centroid $\bar{z}$ with constant angular velocity, and let $R \in SO(d)$ be the transformation matrix from the default reference frame to this rotating one. Let

$$y_i = \bar{z} + R(z_i - \bar{z})$$

be the ith agent's coordinates in the rotating reference frame. Suppose that R is chosen such as $\dot{R} = RA$; then, it is easy to rewrite the swarm centroid and the interagent distances in terms of the new coordinates $y_i,\ i = 1, \ldots, n$, as

$$\frac{1}{n}\sum_{i=1}^{n} y_i = \bar{z} \tag{15}$$

$$y_i - y_j = R(z_i - z_j). \tag{16}$$

TABLE I
SWARM BEHAVIOR

attraction/repulsion term	coupling matrices $\in \mathcal{M}$	behavior	
$g_a(\|\|\cdot\|\|) \geq \alpha$, $g_r(\|\|\cdot\|\|)\|\|\cdot\|\| \leq \beta$	$H^s > 0$	cohesion in $\mathcal{B}(\bar{z}, r)$ $r = \frac{\beta \Delta_{\mathcal{G},\max} \|\|M\|\| \sqrt{n}}{\alpha \lambda_{\min}(H^s) \lambda_2(\mathcal{L}_\mathcal{G})}$	Theorem 1
$g_a(\|\|\cdot\|\|) \geq \alpha$, $g_r(\|\|\cdot\|\|)\|\|\cdot\|\| \leq \beta\|\|\cdot\|\|$	$H^s > 0$ $M^s \geq 0$	cohesion in $\mathcal{B}(\bar{z}, r)$ $r = \sqrt{\frac{\beta \lambda_{max}(M^s)\|E\|}{\alpha \lambda_{min}(H^s) \lambda_2(\mathcal{L}_\mathcal{G})}}$	Theorem 2
...	$H = \mathbb{I}_d$ $M = Q\Lambda Q^T$ $\Lambda = diag(\lambda_1, ..., \lambda_d) \geq 0$	cohesion in a polytopic region	Corollary 1
$g_a(\cdot) = \rho, g_r(\cdot) = 0$	$\omega_A = (\omega_x, \omega_y, \omega_a)^T$ $H = \begin{pmatrix} 0 & -\omega_z & \omega_y \\ \omega_z & 0 & -\omega_x \\ -\omega_y & \omega_x & 0 \end{pmatrix}$ $M = 0$	rotation on planes $\perp \omega_A$	Theorem 3
$g_a(\cdot) = \frac{1}{n}$	$H = S$ $M = S - A$ $S = S^T > 0, A = -A^T$	rotation with rotation axis and angular velocity defined by A	Theorem 4

Note also that $\|y_i - y_j\| = \|z_i - z_j\|$ since R is a rotation matrix. By using (15) and (16), the evolution of the ith agent, w.r.t. the chosen rotating reference frame, becomes

$$\dot{y}_i(t) = -\sum_{j=1}^{n} \left[g_a(||y_i - y_j||) RHR^T - \frac{1}{n} RAR^T \right] (y_i - y_j) + RMR^T \sum_{j=1}^{n} g_r(||y_i - y_j||)(y_i - y_j).$$

Considering the assumptions on M and H, the first term can be rearranged to obtain

$$\dot{y}_i(t) = -\sum_{j=1}^{n} \left[\frac{1}{n} - g_r(||y_i - y_j||) \right] RMR^T (y_i - y_j). \quad (17)$$

Now, by defining $Q = RM^{-1}R^T$, the agent evolution can be recast in

$$Q\dot{y}_i = -\frac{1}{n} \sum_{j=1}^{n} (y_i - y_j) + \sum_{j=1}^{n} g_r(||y_i - y_j||)(y_i - y_j). \quad (18)$$

Utilizing Assumption 3, (18) can be rewritten as

$$Q\dot{y}_i = -\sum_{j=1,\ i \neq j}^{n} \left[\frac{1}{2n} \nabla_{y_i} (||y_i - y_j||^2) - \nabla_{y_i} J_r(||y_i - y_j||) \right].$$

Since $Q^s > 0$, the agents tend to stationary positions (see [3, Th. 1, p. 33]). This means that agents converge to a constant configuration w.r.t. the rotating reference frame, and then, they start rotating with constant angular velocity (defined by the matrix A) around the swarm centroid. ■

Remark 6: It is straightforward to conclude that if the angular velocity is zero along all the axes, then the agents will reach a steady-state constant configuration w.r.t. $\bar{z}$.

Remark 7: Note here that, as before, the skew-symmetric matrix A determines the rotational (angular motion) behavior of the swarm. Therefore, as was the case in the previous subsection, A can be chosen based on the desired axis, direction, and speed of rotation. In contrast, the symmetric and positive-definite matrix S together with A (and the attraction/repulsion function) affect the aggregation behavior of the swarm. Therefore, S can be chosen based on the desired aggregation characteristics.

For the sake of the reader, Table I summarizes the swarm behavior based on the choice of coupling matrices.

V. NUMERICAL SIMULATIONS

In this section, the effectiveness of the proposed model is shown by means of simulations on a team of agents moving in the 3-D space. The proposed simulations represent the main characteristics of the model, which differentiates it from the one proposed in [1].

A. Example 1

This example aims to show the capability of the matrix M to determine the final configuration of the swarm. The attraction/repulsion function $g(\cdot)$ with linear attraction and unbounded repulsion is used in the simulation with

$$g_a(||y||) = 1,\ g_r(||y||) = 1/||y||^2.$$

Note that these functions satisfy Assumptions 1–3 with $J_a = (1/2)\|x\|^2$ and $J_r = \ln(\|x\|)$. Assume that there are ten agents in the swarm, which are required to create a formation on the xz plane passing through the swarm centroid. This is done by choosing the coordinate-coupling matrices as

$$H = \mathbb{I}_3$$

and, for example

$$M = \begin{pmatrix} 1 & 0 & 0 \\ 0 & 0 & 0 \\ 0 & 0 & 2 \end{pmatrix}.$$

With this choice and according to Corollary 1, the agents, as shown in Fig. 1, tend to enter the polytopic region and then to reduce the y-component of their distance from the centroid. This is guaranteed by the null eigenvalue of the matrix M.

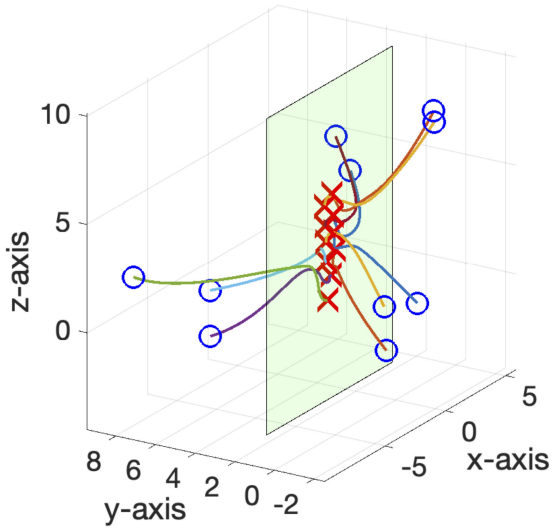

Fig. 1. Example 1: Agents' trajectories. Initial (blue circles) and final (red crosses) positions.

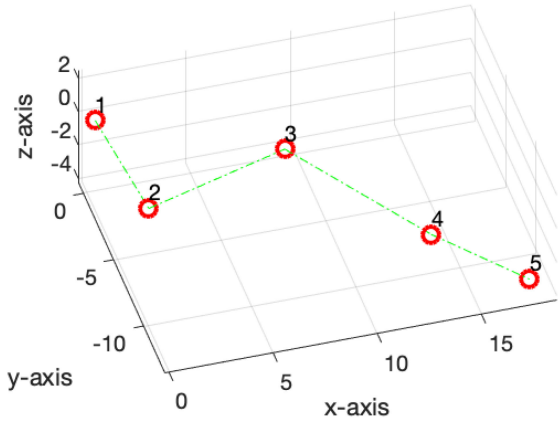

Fig. 2. Example 2: Agents' initial positions. Graph connectivity.

TABLE II
EXAMPLE 3: INITIAL CONDITIONS

Agent	x	y	z
1	0.63	0.81	-0.75
2	1.99	-3.33	-3.03
3	7.37	-7.29	2.42
4	12.59	-13.52	1.05
5	17.82	-11.75	-4.23

B. Example 2

The rotation behavior of the swarm according to the model (13) is here considered. The swarm is composed of five agents initially organized as the connected graph shown in Fig. 2 with initial conditions reported in Table II.

The angular velocity vector is $\omega_A = [1, -2, 3]^T$, while the parameter $\rho = 10$. As evident in Fig. 3, there is no displacement of the agents along the direction parallel to the axis of rotation defined by the vector ω_A, and the movement takes place on planes perpendicular to ω_A.

The obtained trajectories, as expected, are signals containing harmonics at frequencies $\rho\lambda_k(\mathcal{L}_\mathcal{G})||\omega_A||,\ k = 2, \ldots, 5$, i.e.,

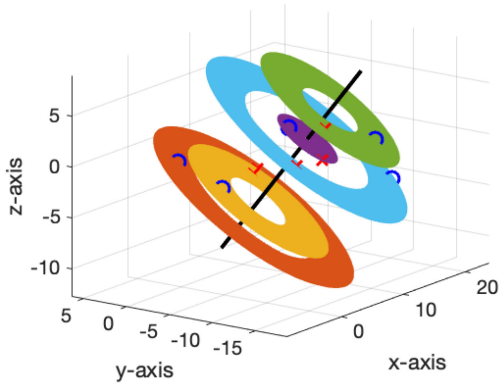

Fig. 3. Example 2: Agents' trajectories. Initial (blue circles) and final (red crosses) positions. Axis of rotation (black line).

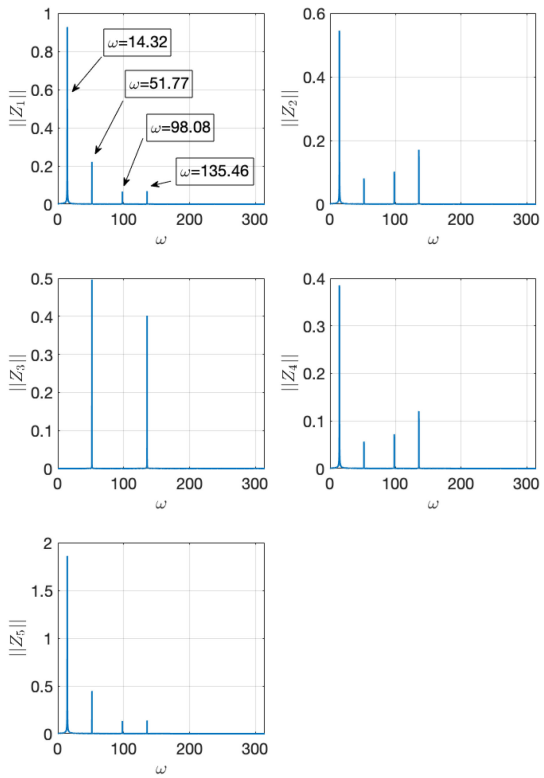

Fig. 4. Example 2: Discrete Fourier transform of $z_i^\perp(t),\ i = 1, \ldots, 5$.

(14.3, 51.7, 97.9, 135.4). A Fourier analysis is then conducted on $z_i(t),\ i = 1, \ldots, 5$, to find the harmonics of the signals. Fig. 4 shows the norm of the discrete Fourier transform of z_i, namely, $||Z_i||$, (where the dc frequency is removed for the sake of readability) for all the agents w.r.t. the angular frequency ω. As shown, for example, in the case of $||Z_1||$, the signal $z_1(t)$ contains all the frequencies $\rho\lambda_k(\mathcal{L}_\mathcal{G})||\omega_A||,\ k = 2, \ldots, 5$.

C. Example 3

In this example, the rotational behavior exhibited by the proposed kinematic model, in the case of complete connectivity, is highlighted. A swarm with 20 agents is considered with the

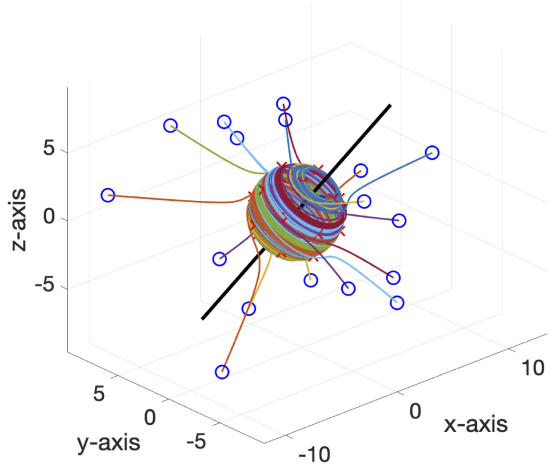

Fig. 5. Example 3: Agents' trajectories. Initial (blue circles) and final (red crosses) positions. Axis of rotation (black line).

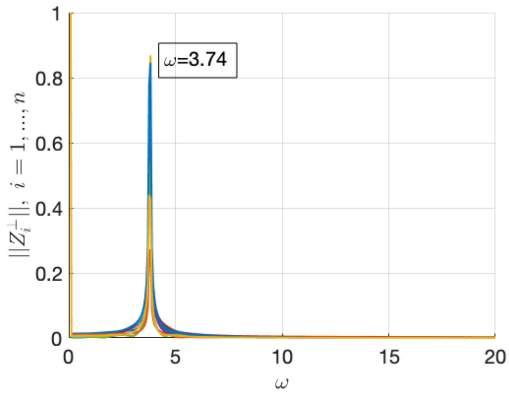

Fig. 6. Example 3: Discrete Fourier transform of $z_i^{\perp}(t),\ i = 1, \ldots, 20$.

attractive term $g_a(||y||) = 1/20$ and the unbounded repulsive term $g_r(||y||) = \frac{1}{||y||^2}$.

The angular velocity vector is chosen as $\omega_A = [1, -2, 3]^T$. The matrix S is set as $10\mathbb{I}_3$. As expected, according to Theorem 4, the agents reach a rotating behavior that can be better understood by taking a look at Fig. 5, which depicts the agents initial positions (blue circles), the evolutions in terms of their components, and the axis of rotation (black line) parallel to ω_A passing through the stationary centroid of the swarm.

In order to test that the angular velocity of the agents around the rotational axis is compliant with the magnitude of the vector ω_A, the following arguments are exploited. First, note that the position of the ith agent can be decomposed into two components $z_i^{||}(t)$ and $z_i^{\perp}(t)$, which are parallel and perpendicular to ω_A, respectively. In particular, the latter component can be computed as $z_i^{\perp}(t) = \left(\mathbb{I}_3 - \frac{\omega_A \omega_A^T}{||\omega_A||^2}\right) z_i(t)$. A Fourier analysis is then conducted on $z_i^{\perp}(t)$ to find the principal component of the angular velocity. Fig. 6 shows the norm of the discrete Fourier transform of $z_i^{\perp}(t)$, namely, $||Z_i^{\perp}||$ (normalized on the dc component) for all the agents w.r.t. the angular frequency ω. As evident, each agent rotates with angular frequency equal to the magnitude of ω_A.

VI. Conclusion

In this article, an extension to the swarm model of Gazi and Passino was presented. The model has the advantage to permit the aggregation and rotation of the agents around the swarm centroid. This favorable behavior is then able to imitate certain biological species performing rotating group movements. The characteristics of this behavior can be tuned by properly choosing two coordinate-coupling matrices weighting both the attraction and repulsion functions. Numerical simulations were presented to illustrate the characteristics of the swarm model. Potential extensions of the work may include incorporating higher order agent dynamics, analyzing the kinetic and potential energy properties of the agent interactions (swarm dynamics), and considering consensus-based emergent axis of rotation.

References

[1] V. Gazi and K. M. Passino, "A class of attractions/repulsion functions for stable swarm aggregations," *Int. J. Control*, vol. 77, no. 18, pp. 1567–1579, 2004.
[2] W. Ren and Y. Cao, *Distributed Coordination of Multi-Agent Networks: Emergent Problems, Models, and Issues*. Berlin, Germany: Springer, 2010.
[3] V. Gazi and K. M. Passino, *Swarm Stability and Optimization*. Berlin, Germany: Springer, 2011.
[4] R. Olfati-Saber, J. A. Fax, and R. M. Murray, "Consensus and cooperation in networked multi-agent systems," *Proc. IEEE*, vol. 95, no. 1, pp. 215–233, Jan. 2007.
[5] L. Wang and F. Xiao, "Finite-time consensus problems for networks of dynamic agents," *IEEE Trans. Autom. Control*, vol. 55, no. 4, pp. 950–955, Apr. 2010.
[6] S. Li, H. Du, and X. Lin, "Finite-time consensus algorithm for multi-agent systems with double-integrator dynamics," *Automatica*, vol. 47, no. 8, pp. 1706–1712, 2011.
[7] M. Maghenem, A. Loría, and E. Panteley, "A cascades approach to formation-tracking stabilization of force-controlled autonomous vehicles," *IEEE Trans. Autom. Control*, vol. 63, no. 8, pp. 2662–2669, Aug. 2018.
[8] B. A. Francis and M. Maggiore, *Flocking and Rendezvous in Distributed Robotics*. Berlin, Germany: Springer, 2016.
[9] N. T. Binh, P. D. Dai, N. H. Quang, N. T. Ty, and N. M. Hung, "Flocking control for two-dimensional multiple agents with limited communication ranges," *Int. J. Control*, vol. 94, no. 9, pp. 2411–2418, 2021.
[10] G. Fedele and L. D'Alfonso, "A kinematic model for swarm finite-time trajectory tracking," *IEEE Trans. Cybern.*, vol. 49, no. 10, pp. 3806–3815, Oct. 2019.
[11] J. Yao, R. Ordonez, and V. Gazi, "Swarm tracking using artificial potentials and sliding mode control," *J. Dyn. Syst., Meas. Control*, vol. 129, no. 5, pp. 749–754, 2007.
[12] N. Michael, J. Fink, S. Loizou, and V. Kumar, "Architecture, abstractions, and algorithms for controlling large teams of robots: Experimental testbed and results," in *Robotics Research*. Berlin, Germany: Springer, 2010, pp. 409–419.
[13] O. Khatib, "Real-time obstacle avoidance for manipulators and mobile robots," in *Autonomous Robot Vehicles*, I. Cox and G. Wilfong, Eds. Berlin, Germany: Springer, 1986, pp. 396–404.
[14] H. G. Tanner, G. J. Pappas, and V. Kumar, "Leader-to-formation stability," *IEEE Trans. Robot. Autom.*, vol. 20, no. 3, pp. 443–455, Jun. 2004.
[15] R. Olfati-Saber, "Flocking for multi-agent dynamic systems: Algorithms and theory," *IEEE Trans. Autom. Control*, vol. 51, no. 3, pp. 401–420, Mar. 2006.
[16] A. Jadbabaie, J. Lin, and A. S. Morse, "Coordination of groups of mobile autonomous agents using nearest neighbor rules," *IEEE Trans. Autom. Control*, vol. 48, no. 6, pp. 988–1001, Jun. 2003.
[17] H. Su, X. Wang, and Z. Lin, "Flocking of multi-agents with a virtual leader," *IEEE Trans. Autom. Control*, vol. 54, no. 2, pp. 293–307, Feb. 2009.
[18] J. P. Desai, J. P. Ostrowski, and V. Kumar, "Modeling and control of formations of nonholonomic mobile robots," *IEEE Trans. Robot. Autom.*, vol. 17, no. 6, pp. 905–908, Dec. 2001.

[19] T. Balch and R. C. Arkin, "Behavior-based formation control for multirobot teams," *IEEE Trans. Robot. Autom.*, vol. 14, no. 6, pp. 926–939, Dec. 1998.
[20] Z. Cao, L. Xie, B. Zhang, S. Wang, and M. Tan, "Formation constrained multi-robot system in unknown environments," in *Proc. IEEE Int. Conf. Robot. Autom.*, vol. 1, 2003, pp. 735–740.
[21] M. A. Lewis and K.-H. Tan, "High precision formation control of mobile robots using virtual structures," *Auton. Robots*, vol. 4, no. 4, pp. 387–403, 1997.
[22] R. W. Beard, J. Lawton, and F. Y. Hadaegh, "A coordination architecture for spacecraft formation control," *IEEE Trans. Control Syst. Technol.*, vol. 9, no. 6, pp. 777–790, Nov. 2001.
[23] C. Belta and V. Kumar, "Abstraction and control for groups of robots," *IEEE Trans. Robot.*, vol. 20, no. 5, pp. 865–875, Oct. 2004.
[24] N. Michael, C. Belta, and V. Kumar, "Controlling three dimensional swarms of robots," in *Proc. IEEE Int. Conf. Robot. Autom.*, 2006, pp. 964–969.
[25] A. Bono, G. Fedele, and G. Franzè, "A swarm-based distributed model predictive control scheme for autonomous vehicle formations in uncertain environments," *IEEE Trans. Cybern.*, early access, May 13, 2021, doi: 10.1109/TCYB.2021.3070461.
[26] F. Rossi, S. Bandyopadhyay, M. T. Wolf, and M. Pavone, "Multi-agent algorithms for collective behavior: A structural and application-focused atlas," 2021, *arXiv:2103.11067*.
[27] G. Fedele, L. D'Alfonso, and A. Bono, "Vortex formation in a swarm of agents with a coordinates mixing matrix-based model," *IEEE Control Syst. Lett.*, vol. 4, no. 2, pp. 420–425, Apr. 2020.
[28] C. J. Ingham and E. B. Jacob, "Swarming and complex pattern formation in *Paenibacillus vortex* studied by imaging and tracking cells," *BMC Microbiol.*, vol. 8, no. 1, 2008, Art. no. 36.
[29] E. Lauga, W. R. DiLuzio, G. M. Whitesides, and H. A. Stone, "Swimming in circles: Motion of bacteria near solid boundaries," *Biophys. J.*, vol. 90, no. 2, pp. 400–412, 2006.
[30] S. Childress and E. Spiegel, "Pattern formation in a suspension of swimming microorganisms: Nonlinear aspects," in *A Celebration of Mathematical Modeling*. Berlin, Germany: Springer, 2004, pp. 33–52.
[31] A. Czirók, M. Matsushita, and T. Vicsek, "Theory of periodic swarming of bacteria: Application to Proteus mirabilis," *Phys. Rev. E*, vol. 63, no. 3, 2001, Art. no. 0 31915.
[32] J. Vollmer, A. G. Vegh, C. Lange, and B. Eckhardt, "Vortex formation by active agents as a model for Daphnia swarming," *Phys. Rev. E*, vol. 73, no. 6, 2006, Art. no. 0 61924.
[33] S. Bazazi, K. S. Pfennig, N. O. Handegard, and I. D. Couzin, "Vortex formation and foraging in polyphenic spadefoot toad tadpoles," *Behav. Ecol. Sociobiol.*, vol. 66, no. 6, pp. 879–889, 2012.
[34] N. R. Franks *et al.*, "Social behaviour and collective motion in plant-animal worms," *Proc. Roy. Soc. B: Biol. Sci.*, vol. 283, no. 1825, 2016, Art. no. 20152946.
[35] S. G. Wilson, "Basking sharks (Cetorhinus maximus) schooling in the southern gulf of maine," *Fisheries Oceanogr.*, vol. 13, no. 4, pp. 283–286, 2004.
[36] N. E. Leonard and E. Fiorelli, "Virtual leaders, artificial potentials and coordinated control of groups," in *Proc. IEEE 40th IEEE Conf. Decis. Control*, vol. 3, 2001, pp. 2968–2973.
[37] R. Sepulchre, D. A. Paley, and N. E. Leonard, "Stabilization of planar collective motion: All-to-all communication," *IEEE Trans. Autom. Control*, vol. 52, no. 5, pp. 811–824, May 2007.
[38] W. Ren, "Collective motion from consensus with Cartesian coordinate coupling," *IEEE Trans. Autom. Control*, vol. 54, no. 6, pp. 1330–1335, Jun. 2009.
[39] Y.-Y. Chen, K.-X. Wang, Y. Zhang, C.-L. Liu, and Q. Wang, "A geometric extension design for second-order nonlinear agents formation surrounding a sphere," in *Proc. Chinese Control Decis. Conf.*, 2016, pp. 4868–4873.
[40] X. Ai, Y.-Y. Chen, and Y. Zhang, "Spherical formation tracking of nonholonomic vehicles in three-dimensional space," in *Proc. 11th Asian Control Conf.*, 2017, pp. 1877–1882.
[41] J. Delcourt, N. W. F. Bode, and M. Denoël, "Collective vortex behaviors: Diversity, proximate, and ultimate causes of circular animal group movements," *Quart. Rev. Biol.*, vol. 91, no. 1, pp. 1–24, 2016.
[42] T. Vicsek and A. Zafeiris, "Collective motion," *Phys. Rep.*, vol. 517, no. 3/4,, pp. 71–140, 2012.
[43] M. Mesbahi and M. Egerstedt, *Graph Theoretic Methods in Multiagent Networks*, vol. 33. Princeton, NJ, USA: Princeton Univ. Press, 2010.
[44] A. Baker, *Matrix Groups: An Introduction to Lie Group Theory*. Berlin, Germany: Springer, 2012.
[45] J. Gallier and D. Xu, "Computing exponentials of skew-symmetric matrices and logarithms of orthogonal matrices," *Int. J. Robot. Autom.*, vol. 18, no. 1, pp. 10–20, 2003.

Giuseppe Fedele (Member, IEEE) received the Laurea (M.Sc.) degree (*cum laude*) in computer science engineering and the Ph.D. degree in computer science and system engineering from the University of Calabria, Rende, Italy, in 1999 and 2005, respectively.

Since 2006, he has been an Assistant Professor in Control Engineering with the Department of Informatics, Modeling, Electronics and Systems Engineering, University of Calabria, Rende, Italy. He is a Founding Member of GiPStech s.r.l., a startup and spin-off of the University of Calabria, which develops novel solutions for the indoor localization and navigation problems. His current research interests include power systems, identification and filtering methods, adaptive control, adaptive algorithms for active noise and vibration control, signal processing for localization, navigation, and tracking, and multiagent systems.

Dr. Fedele was the Guest Editor for the Special Issue "Recent Advances in Adaptive Methods for Frequency Estimation with Applications" of the *International Journal of Adaptive Control and Signal Processing* in 2016. He is an Academic Editor for *Mathematical Problems in Engineering*.

Luigi D'Alfonso received the Ph.D. degree in systems and computer engineering from the Department of Informatics, Modeling, Electronics and Systems Engineering, University of Calabria, Rende, Italy, in 2014.

In 2012, he was a Visiting Scholar with the Service d'Automatique et d'Analyse des Systèms, Université Libre de Bruxelles, Bruxelles, Belgium. Since 2015, he has been a Researcher with GiPStech s.r.l., Rende Italy. His current research interests include mobile robots control, localization/mapping/simultaneous localization and mapping for single-agent and multiagent systems, perspective-n-point problem using cameras, and inertial measurements units.

Veysel Gazi (Senior Member, IEEE) received the B.S. degree in electrical and electronics engineering from the Middle East Technical University, Ankara, Turkey, in 1996, and the M.S. and Ph.D. degrees in electrical engineering from the Ohio State University, Columbus, OH, USA, in 1998 and 2002, respectively.

From 1996 to 1997, he was a Scholar of the Scientific and Technological Research Council of Turkey, Ankara, Turkey. He is currently with the Department of Control and Automation Engineering, Faculty of Electrical and Electronics Engineering, Yildiz Technical University, Istanbul, Turkey. He has coauthored many scientific papers. His current research interests include modeling, analysis, and decentralized coordination and control of multiagent dynamical systems.

Dr. Gazi is a recipient (shared with Kevin M. Passino) of the 2005 IEEE Systems, Man, and Cybernetics Society Andy P. Sage Best Transactions Paper Award. He is a coauthor of the books *The RCS Handbook: Tools for Real-Time Control Systems Software Development* (Wiley, 2001) and *Swarm Stability and Optimization* (Springer, 2011). He is a technical publication reviewer for many journals and conferences. He has also served in the technical program committees and in the organizing committees of many respected national or international conferences and as a Guest Editor for *Turkish Journal of Electrical Engineering and Computer Sciences* Special Issue on "Swarm Robotics" published in 2007.